Attittude Determination using Unscented and Extended Kalman Filters

João Filipe Silva
MP-208: Optimal Filtering with Aerospace Applications

December 19, 2020

Abstract

This document contains the final simulation exercise for the Optimal Filtering with Aerospace Applications class. Based on the content given in the lectures, it was requested to formulate an algorithm capable of representing a non-linear dynamic system model whose states were to be estimated by an Extended Kalman Filter and a Unscented Kalman Filter. The estimators were implemented in Matlab scripts[1] and plots were generated to illustrate the estimation errors.

1 Problem Statement

Let $\mathcal{S}_b \triangleq \{B; \hat{x}_b, \hat{y}_b, \hat{z}_b\}$ represent a Cartesian coordinate system (CCS) with its origin on the center of mass of a body. Also, $\mathcal{S}_g \triangleq \{G; \hat{x}_g, \hat{y}_g, \hat{z}_g\}$ represents an inertial CCS with its origin on the ground. Consider a Multirotor Aerial Vehicle (MAV), whose attitude kinematics in Euler angles 1-2-3 can described by:

$$\dot{\alpha}^{b/g} = \mathbf{A}\left(\alpha^{b/g}\right)\omega_b^{b/g} \tag{1}$$

where $\alpha^{b/g} \triangleq [\phi\ \theta\ \psi]^T$ is the vector of Euler angles, $\omega_b^{b/g} \in \mathbb{R}^3$ is the $\mathcal{S}_b$ representation of the angular velocity of $\mathcal{S}_b$ with respect to $\mathcal{S}_g$, and

$$\mathbf{A}\left(\alpha^{b/g}\right) \triangleq \begin{bmatrix} c\psi/c\theta & -s\psi/c\theta & 0 \\ s\psi & c\psi & 0 \\ -c\psi s\theta/c\theta & s\psi s\theta/c\theta & 1 \end{bmatrix} \tag{2}$$

where $cx \triangleq cos(x)$ and $sx \triangleq sin(x)$.

This MAV is equipped with three inertial sensors: a Rate Gyro, an Accelerometer, and a Magnetometer. The Rate Gyro measure $\breve{\omega}_b \in \mathbb{R}^3$ can be modeled by:

$$\breve{\omega}_b = \omega_b^{b/g} + \beta_b^{gy} + \mathbf{w}_b^{gy} \tag{3}$$

where $\mathbf{w}_b^{gy} \in \mathbb{R}^3$ is a zero-mean white Gaussian noise with covariance $\mathbf{Q}^{gy}$, which, for simplicity, is assumed constant and known; and $\beta_b^{gy} \in \mathbb{R}^3$ is a drifting bias described by the following Wiener process:

$$\dot{\beta}_b^{gy} = \mathbf{w}_b^{d,gy} \tag{4}$$

where $\mathbf{w}_b^{d,gy}$ is assumed to be a zero-mean white Gaussian noise with knows covariance $\mathbf{Q}^{d,gy}$.

[1]All scripts can be found in: https://github.com/jfilipe33/ExCompMP208

The accelerometer measure $\check{\mathbf{a}}_b \in \mathbb{R}^3$ can be modeled by

$$\check{\mathbf{a}}_b = \mathbf{D}^{b/g}\left(\dot{\mathbf{v}}_g^{b/g} - \mathbf{g}_g\right) + \mathbf{w}_b^{ac} \tag{5}$$

where $\mathbf{D}^{b/g}$ represents the attitude matrix of $\mathcal{S}_b$ with respect to $\mathcal{S}_g$, $\mathbf{g}_g \triangleq -g\mathbf{e}_3$ is the gravity acceleration vector[2], and $\mathbf{w}_b^{ac} \in \mathbb{R}^3$ is assumed to be a zero-mean white Gaussian noise with known covariance $\mathbf{Q}^{ac}$. Matrix $\mathbf{D}^{b/g}$ can be calculated, in Euler angles 1-2-3, by:

$$\mathbf{D}^{b/g} = \begin{bmatrix} c\psi c\theta & c\psi s\theta s\phi + s\psi c\phi & -c\psi s\theta c\phi + s\psi s\phi \\ -s\psi c\theta & -s\psi s\theta s\phi + c\psi c\phi & s\psi s\theta c\phi + c\psi s\phi \\ s\theta & -c\theta s\phi & c\theta c\phi \end{bmatrix}. \tag{6}$$

To simplify, assume that $\dot{\mathbf{v}}_g^{b/g} = 0$ throughout the experiment.

The magnetometer measure $\check{\mathbf{m}}_b \in \mathbb{R}^3$ can be modeled by

$$\check{\mathbf{m}}_b = \mathbf{D}^{b/g}\mathbf{m}_g + \mathbf{w}_b^{mg} \tag{7}$$

where $\mathbf{m}_g \in \mathbb{R}^3$ is the $\mathcal{S}_g$ representation of the local magnetic field and $\mathbf{w}_b^{mg} \in \mathbb{R}^3$ is assumed to be a zero-mean white Gaussian noise with known covariance $\mathbf{Q}^{mg}$. To simplify, assume that $\mathbf{m}_g$ keeps constant throughout the experiment.

Equations (1)-(7) can be put together in the following state and measurement equations

$$\begin{aligned} \dot{\mathbf{x}}(t) &= \mathbf{f}\left(\mathbf{x}(t), u(t)\right) + \mathbf{G}(\mathbf{x})\mathbf{w}(t) \\ y_{k+1} &= h\left(\mathbf{x}_{k+1}\right) + v_{k+1} \end{aligned} \tag{8}$$

where $\mathbf{x}(t) \triangleq \left[\left(\alpha^{b/g}\right)^T \ \left(\beta_b^{gy}\right)^T\right]^T \in \mathbb{R}^6$, $u(t) \triangleq \check{\omega}_b \in \mathbb{R}^3$, $\mathbf{w}(t) \triangleq \left[\left(\mathbf{w}_b^{gy}\right)^T \ \left(\mathbf{w}_b^{d,gy}\right)^T\right]^T \in \mathbb{R}^6$, and

$$\begin{aligned} \mathbf{f}\left(\mathbf{x}(t), u(t)\right) &\triangleq \begin{bmatrix} \mathbf{A}\left(\alpha^{b/g}\right)\left(\check{\omega}_b - \beta_b^{gy}\right) \\ \mathbf{0}_{3\times 1} \end{bmatrix} \in \mathbb{R}^6 \\ \mathbf{G}(\mathbf{x}) &\triangleq \begin{bmatrix} -\mathbf{A}\left(\alpha^{b/g}\right) & \mathbf{0}_{3\times 3} \\ \mathbf{0}_{3\times 3} & \mathbf{I}_3 \end{bmatrix} \in \mathbb{R}^{6\times 6} \end{aligned}$$

The measurement equation in (8), when normalized by the factors g and $||\mathbf{m}_g||$, can be dismembered as:

$$\mathbf{y}_k \triangleq \begin{bmatrix} \check{\mathbf{a}}_b/g \\ \check{\mathbf{m}}_b/||\mathbf{m}_g|| \end{bmatrix}, \quad \mathbf{h}(\mathbf{x}_k) \triangleq \begin{bmatrix} \mathbf{D}(\alpha^{b/g})\mathbf{e}_3 \\ \mathbf{D}(\alpha^{b/g})\frac{\mathbf{m}_g}{||\mathbf{m}_g||} \end{bmatrix}, \quad \mathbf{v}_k \triangleq \begin{bmatrix} \mathbf{w}_b^{ac}/g \\ \mathbf{w}_b^{mg}/||\mathbf{m}_g|| \end{bmatrix}$$

This normalization is made to avoid numerical problems in the computer simulation. For the sake of convenience, consider the following angular velocity signal as a forcing function:

$$\omega_b^{b/g}(k) = \frac{2\pi}{20}\begin{bmatrix} sin(0.5\pi T_s k) \\ sin(0.5\pi T_s k + 0.5\pi) \\ sin(0.5\pi T_s k + \pi) \end{bmatrix} \tag{9}$$

Adopt the parameters presented in Table 1.

The goal of this exercise is to present the estimation errors of the states $\mathbf{x}(t)$, using an Extended Kalman Filter and a Unscented Kalman Filter.

[2] $\mathbf{e}_1 = [1\ 0\ 0]^T$, $\mathbf{e}_2 = [0\ 1\ 0]^T$, $\mathbf{e}_3 = [0\ 0\ 1]^T$

Table 1: System Parameters

Description	Value
Initial Conditions of the plant	$\begin{bmatrix} \alpha^{b/g}(0) \\ \beta_b^{gy}(0) \end{bmatrix} \sim \mathcal{N}(\mathbf{0}_{6\times 1}, diag((\pi/9)^2\mathbf{I}_3, 10^{-1}\mathbf{I}_3))$
Rate-gyro noise	$\mathbf{Q}^{gy} = 2.5 \times 10^{-7}\mathbf{I}_3$
Rate-gyro drift	$\mathbf{Q}^{d,gy} = 1.0 \times 10^{-12}\mathbf{I}_3$
Accelerometer noise	$\mathbf{Q}^{ac} = 1.5 \times 10^{-5}\mathbf{I}_3$
Magnetometer noise	$\mathbf{Q}^{mg} = 2 \times 10^{-2}\mathbf{I}_3\ \mu T$
Local magnetic field	$\mathbf{m}_g = [13.7 \quad -4.6 \quad -10.9]^T\ \mu T$
Gravity acceleration	$g = 9.81\ m/s^2$
Sensor sampling time	$T_s = 0.01s$

2 Extended Kalman Filter (EKF)

A Kalman Filter uses a Minimum Mean Square Error estimator to estimate the state at the current instant k, given the measurements obtained since the start of the simulation until the instant k. For non-linear systems and noises not necessarily normally distributed, an approximately optimal estimator can be calculated using the Extended Kalman Filter. Equations (1)-(3) show a non-linear continuous system, with $\mathbf{f}$ and h differentiable.

Approximate the non-linear functions $\mathbf{f}$ and $\mathbf{h}$ by Taylor series expansion and truncation:

$$\mathbf{f}\left(\mathbf{x}(t), \mathbf{u}(t)\right) \approx \mathbf{f}\left(\hat{\mathbf{x}}(t), \mathbf{u}(t)\right) + \mathbf{F}(t)\left(\mathbf{x}(t) - \hat{\mathbf{x}}(t)\right) \tag{10}$$

$$\mathbf{g}\left(\mathbf{x}(t)\right) \approx \mathbf{g}\left(\hat{\mathbf{x}}(t)\right) \triangleq \mathbf{G}(t) \tag{11}$$

$$\mathbf{h}_{k+1}(\mathbf{x}_{k+1}) \approx \mathbf{h}_{k+1}\left(\hat{\mathbf{x}}_{k+1|k}\right) + \mathbf{H}_{k+1}\left(\mathbf{x}_{k+1} - \hat{\mathbf{x}}_{k+1|k}\right) \tag{12}$$

where $\hat{\mathbf{x}}(t) \triangleq E(\mathbf{x}(t)|\mathbf{Y}_{1:k})$, $\hat{\mathbf{x}}_{k+1|k} \triangleq E(\mathbf{x}_{k+1}|\mathbf{Y}_{1:k})$, and

$$\mathbf{F}(t) \triangleq \frac{\partial \mathbf{f}(\hat{\mathbf{x}}(t), u(t))}{\partial \mathbf{x}}, \quad \mathbf{H}_{k+1} \triangleq \frac{d\mathbf{h}_{k+1}(\hat{\mathbf{x}}_{k+1|k})}{d\mathbf{x}}$$

Using (10)-(12), system (8) can be approximated to:

$$\dot{\mathbf{x}}(t) = \mathbf{F}(t)\mathbf{x}(t) + \mathbf{G}(t)\mathbf{w}(t) + \left(\mathbf{f}(\hat{\mathbf{x}}(t), u(t)) - \mathbf{F}(t)\hat{\mathbf{x}}(t)\right) \tag{13}$$

$$\mathbf{y}_{k+1} = \mathbf{H}_{k+1}\mathbf{x}_{k+1} + \mathbf{v}_{k+1} + \left(\mathbf{h}_{k+1}(\hat{\mathbf{x}}_{k+1|k}) - \mathbf{H}_{k+1}\hat{\mathbf{x}}_{k+1|k}\right) \tag{14}$$

Structuring the solution as a recursive algorithm, each iteration will be divided in two steps:

- **Prediction:** the use of (13) and (14) to obtain a predictive estimate;
- **Update:** The fusion of a new measure with the predictive estimate to obtain a filtered estimate.

Given the filtered mean $\hat{\mathbf{x}}_{k|k}$ and the covariance $\mathbf{P}_{k|k}$, The predictive estimate and its covariance are given by integrating the ODEs:

$$\dot{\hat{\mathbf{x}}}(t) = \mathbf{f}(\hat{\mathbf{x}}(t), u(t)) \tag{15}$$

$$\dot{\mathbf{P}}(t) = \mathbf{F}(t)\mathbf{P}(t) + \mathbf{P}(t)\mathbf{F}(t)^T + \mathbf{G}(t)\mathbf{Q}(t)\mathbf{G}(t)^T \tag{16}$$

from t_k to t_{k+1}, considering $u(t) = u_k, \forall t \in [t_k, t_{k+1})$.

Setting $\hat{\mathbf{x}}_{\mathbf{k+1|k}} = \dot{\hat{\mathbf{x}}}(t)$ and $\mathbf{P}_{k+1|k} = \dot{\mathbf{P}}(t)$, it is also possible to obtain the predictive measure, its corresponding conditional covariance, and the conditional cross-covariance between $\mathbf{X}_{k+1}$ and $\mathbf{Y}_{k+1}$ by calculating:

$$\hat{\mathbf{y}}_{k+1|k} = \mathbf{h}_{k+1}(\hat{\mathbf{x}}_{k+1|k}) \tag{17}$$

$$\mathbf{P}^{Y}_{k+1|k} = \mathbf{H}_{k+1}\mathbf{P}_{k+1|k}\mathbf{H}^{T}_{k+1} + \mathbf{R}_{k+1} \tag{18}$$

$$\mathbf{P}^{XY}_{k+1|k} = \mathbf{P}_{k+1|k}\mathbf{H}^{T}_{k+1} \tag{19}$$

Now, for the Update step, the filtered estimate and the estimation error covariance are calculated by:

$$\hat{\mathbf{x}}_{k+1|k+1} = \hat{\mathbf{x}}_{\mathbf{k+1|k}} + \mathbf{K}_{k+1}\left(\mathbf{y}_{k+1} - \hat{\mathbf{y}}_{k+1|k}\right) \tag{20}$$

$$\mathbf{P}_{k+1|k+1} = \mathbf{P}_{k+1|k} - \mathbf{P}^{XY}_{k+1|k}\left(\mathbf{P}^{Y}_{k+1|k}\right)^{-1}\left(\mathbf{P}^{XY}_{k+1|k}\right)^{-1} \tag{21}$$

where $\mathbf{K}_{k+1}$ is the Extended Kalman gain given by

$$\mathbf{K}_{k+1} = \mathbf{P}^{XY}_{k+1|k}\left(\mathbf{P}^{Y}_{k+1|k}\right)^{-1} \tag{22}$$

2.1 EKF Simulations

Before describing the simulations, it is important to declare the Jacobians present in equations (10) and (12). $\mathbf{F}(t)$ was calculated by deriving the vector $\mathbf{f}(\mathbf{x}(t), u(t))$, resulting in:

$$\mathbf{F} = \frac{\partial \mathbf{f}(\mathbf{x}, u)}{\partial \mathbf{x}} = \begin{bmatrix} \mathbf{f}' & -\mathbf{A}(\alpha^{b/g}) \\ \mathbf{0}_{3\times3} & \mathbf{0}_{3\times3} \end{bmatrix} \tag{23}$$

where

$$\mathbf{f}' = \begin{bmatrix} 0 & \frac{c\psi s\theta}{c^2\theta}u_1 - \frac{s\psi s\theta}{c^2\theta}u_2 & \frac{-s\psi}{c\theta}u_1 - \frac{c\psi}{c\theta}u_2 \\ 0 & 0 & c\psi u_1 - s\psi u_2 \\ 0 & \frac{-c\psi}{c^2\theta}u_1 + \frac{s\psi}{c^2\theta}u_2 & \frac{s\psi s\theta}{c\theta}u_1 + \frac{c\psi s\theta}{c\theta}u_2 \end{bmatrix}$$

Similarly, $\mathbf{H}_{k+1}$ was calculated by deriving the vector $\mathbf{h}_{k+1}(\hat{\mathbf{x}}_{k+1|k})$, resulting in

$$\mathbf{H} = \frac{d\mathbf{h}_{k+1}(\hat{\mathbf{x}}_{k+1|k})}{d\mathbf{x}} = \begin{bmatrix} \frac{\partial \mathbf{D}}{\partial \phi}\mathbf{e}_3 & \frac{\partial \mathbf{D}}{\partial \theta}\mathbf{e}_3 & \frac{\partial \mathbf{D}}{\partial \psi}\mathbf{e}_3 & \mathbf{0}_{3\times3} \\ \frac{\partial \mathbf{D}}{\partial \phi}\frac{\mathbf{m}_g}{||\mathbf{m}_g||} & \frac{\partial \mathbf{D}}{\partial \theta}\frac{\mathbf{m}_g}{||\mathbf{m}_g||} & \frac{\partial \mathbf{D}}{\partial \psi}\frac{\mathbf{m}_g}{||\mathbf{m}_g||} & \mathbf{0}_{3\times3} \end{bmatrix} \tag{24}$$

where

$$\frac{\partial \mathbf{D}}{\partial \phi} = \begin{bmatrix} 0 & c\psi s\theta c\phi - s\psi s\phi & c\psi s\theta s\phi + s\psi c\phi \\ 0 & -s\psi s\theta c\phi - c\psi s\phi & -s\psi s\theta s\phi + c\psi c\phi \\ 0 & -c\theta c\phi & -c\theta s\phi \end{bmatrix}$$

$$\frac{\partial \mathbf{D}}{\partial \theta} = \begin{bmatrix} -c\psi s\theta & c\psi c\theta s\phi & -c\psi c\theta c\phi \\ s\psi s\theta & -s\psi c\theta s\phi & s\psi c\theta c\phi \\ c\theta & s\theta s\phi & -s\theta c\phi \end{bmatrix}$$

$$\frac{\partial \mathbf{D}}{\partial \psi} = \begin{bmatrix} -s\psi c\theta & -s\psi s\theta s\phi + c\psi c\phi & s\psi s\theta c\phi + c\psi s\phi \\ -c\psi c\theta & -c\psi s\theta s\phi - s\psi c\phi & c\psi s\theta c\phi - s\psi s\phi \\ 0 & 0 & 0 \end{bmatrix}$$

Next, the Extended Kalman Filter was implemented on 100 realizations of the system performance, described by equation (1). Through equations (15)-(22), assuming the initial estimation states $\mathbf{x}_{1|1} = \bar{\mathbf{x}}$ and initial estimation error covariance $\mathbf{P}_{1|1} = \bar{\mathbf{P}}$, the estimation errors obtained are illustrated in Figures 1a to 1f.

The matrix $P_{k|k}$, updated along with the states estimation every iteration, represents the covariance matrix of the estimation error. Therefore, its square root represents the standard deviation matrix of the estimation error. The calculation the matrix square root of $P_{k|k}$ was also plotted in Figures 1a to 1f as red thick dashed lines.

From Figures 1a to 1c, it is possible to see that error estimations don't always converge to zero and stay mainly outside of the envelope formed by the standard deviation lines. In a linear Gaussian system simulation, every estimation error realization should vary inside the limits drawn by the red dashed lines. However, as these are approximately optimal estimations, this result might demand the tuning of the covariance matrices.

2.2 EKF with tuned matrices

Through extensive trial and error, altering matrix $\mathbf{R}$ used to calculate the filter (see equation (18)) to $\mathbf{R}_{ekf} = blkdiag(100 \times \mathbf{Q}^{ac}, 0.1 \times \mathbf{Q}^{mg})$, provided the plots illustrated in figures 2a and 2f.

The goal of this tuning was to reduce the weight of the measurements on the process of estimation, increasing the covariance of the accelerometer measurement and making it less reliable. By changing the reliability of the measurements, the designer intends to force the filter to trust more in its state estimation than its measurements.

This attempt of linearizing a very non-linear system of equations (due to the trigonometric functions), causes the Euler angles estimation errors to rapidly converge, as seen by the red dashed lines almost instantly settling at their stationary value. The same can't be said about the behaviour of the Rate-Gyro bias estimation errors, as its standard deviation lines accomodate smoothly at their stationary value. Another effect of this linearization is that it makes the estimations behave non-gaussianly, turning invalid some desired properties like the grouping of 68% of the samples inside the standard deviation bounds.

It is important to note that the Extended Kalman Filter algorithm took approximately 65 seconds to run the full system simulation and state estimation.

3 Unscented Kalman Filter

In an attempt to improve the performance of estimation of states passing through non-linear systems, researchers studied better ways to linearly approximate said systems. The Extended Kalman Filter does this by using Taylor Series truncation and derivatives to approximate the non-linear function around the mean of the original distribution. Although the original distribution does not need to be Gaussian, it needs to be at least symmetric around its peak probability. The Unscented Kalman Filter uses the mean and multiple other points of the original distribution to make this linear approximation. These points are denominated Sigma Points.

Besides the mean of the *a Posteriori* distribution, the Sigma Point are calculated in pairs

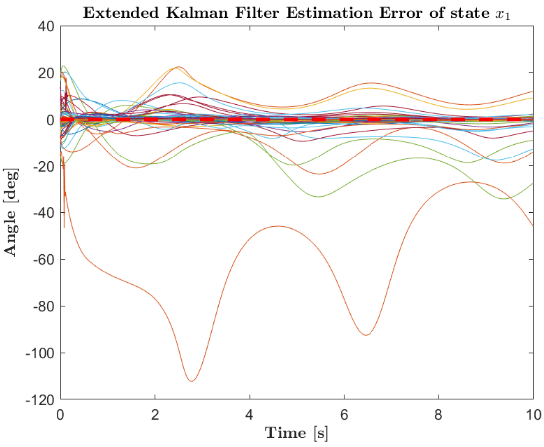

(a) $\tilde{x}_1$

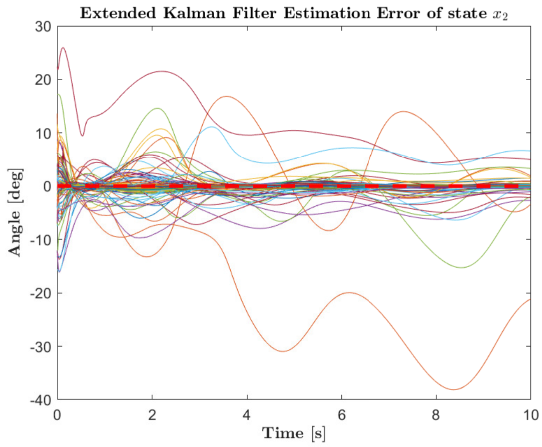

(b) $\tilde{x}_2$

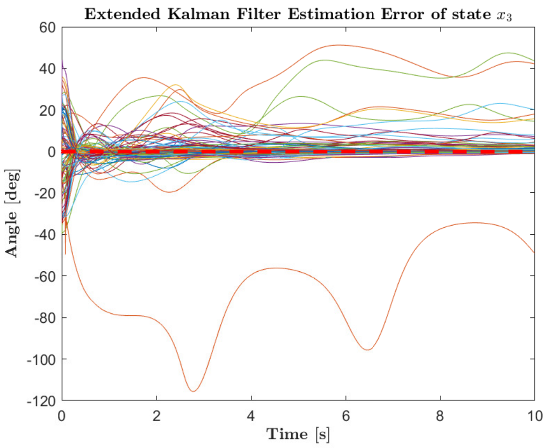

(c) $\tilde{x}_3$

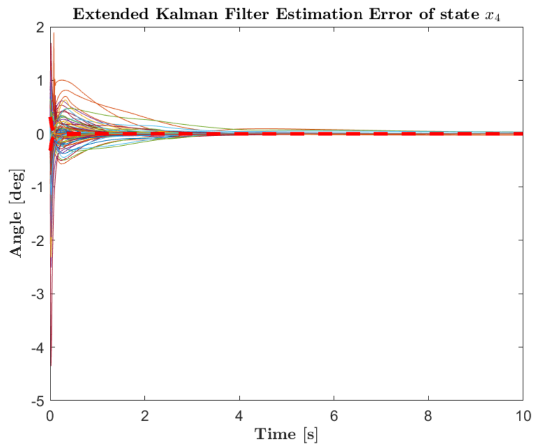

(d) $\tilde{x}_4$

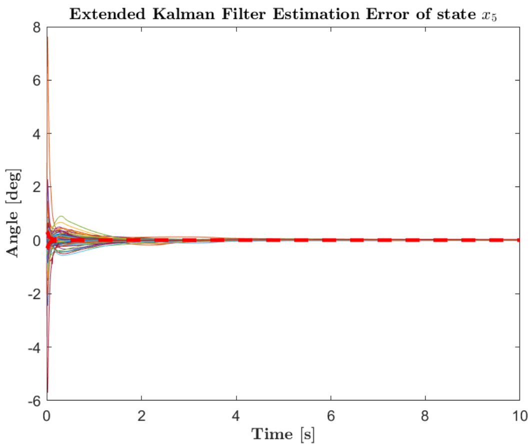

(e) $\tilde{x}_5$

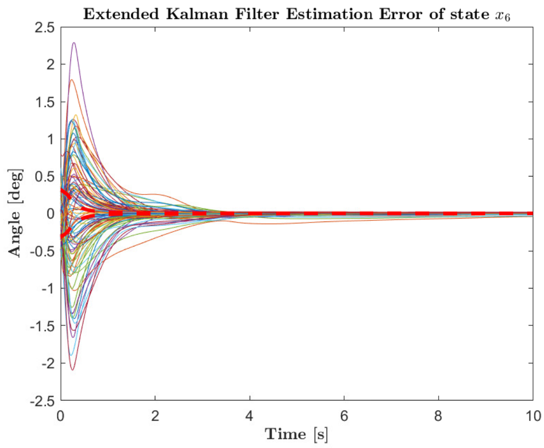

(f) $\tilde{x}_6$

Figure 1: Estimation Error of States x_1 to x_6 with an Extended Kalman Filter

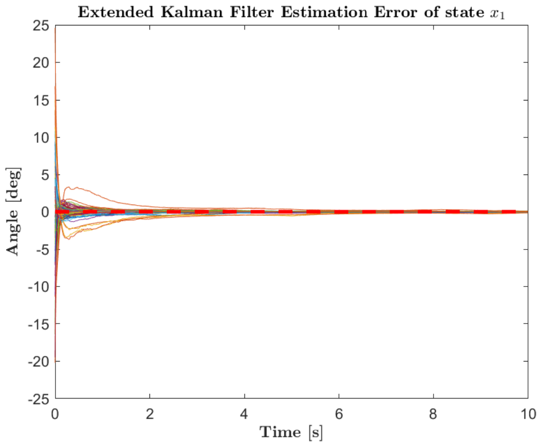

(a) $\tilde{x}_1$

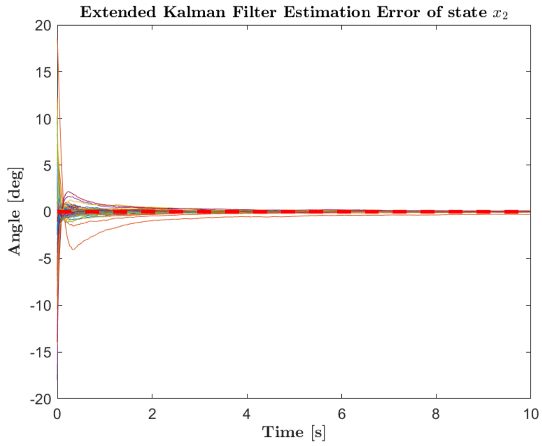

(b) $\tilde{x}_2$

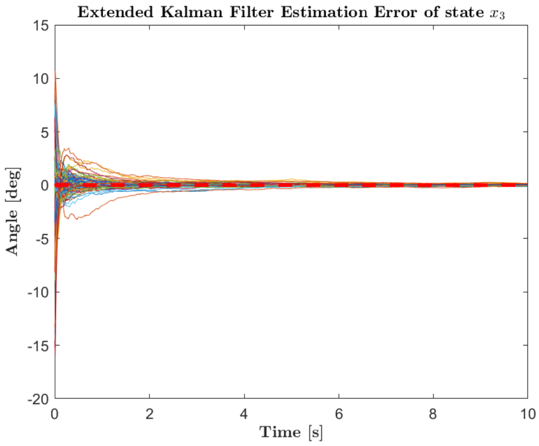

(c) $\tilde{x}_3$

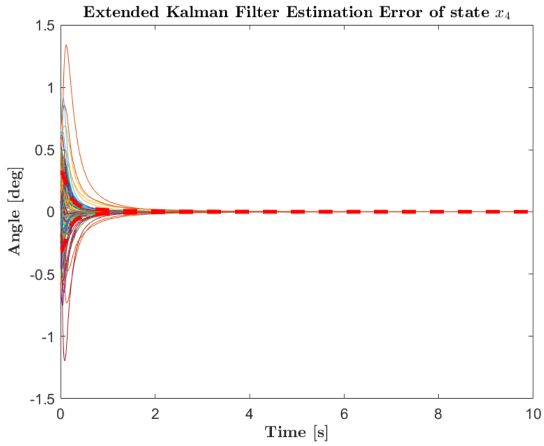

(d) $\tilde{x}_4$

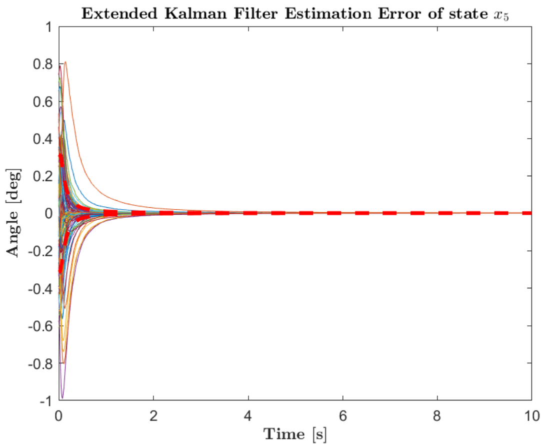

(e) $\tilde{x}_5$

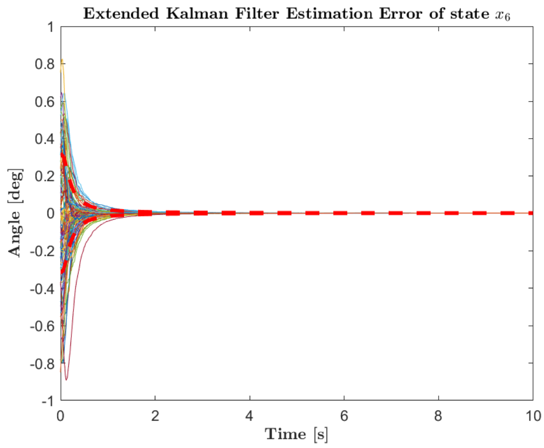

(f) $\tilde{x}_6$

Figure 2: Estimation Error of States x_1 to x_6 with an Extended Kalman Filter and a modified $\mathbf{R}$ matrix.

symmetrically around this mean. Assuming the test system in this report, consider an augmented vector described by

$$
{}^{a}\mathbf{X}(t_k) \triangleq \begin{bmatrix} \mathbf{X}(t_k) \\ \mathbf{W}(t_k) \\ \mathbf{V}_{k+1} \end{bmatrix} \in \mathbb{R}^{n_a} \tag{25}
$$

where $n_a \triangleq n_x + n_w + n_y$.

The mean and covariance of the augmented vector ${}^{a}\mathbf{X}(t_k)$ are given by

$$
{}^{a}\bar{\mathbf{x}}(t_k) \triangleq \begin{bmatrix} \hat{\mathbf{x}}_{k|k} \\ \mathbf{0}_{n_w \times 1} \\ \mathbf{0}_{n_y \times 1} \end{bmatrix}, \quad {}^{a}\mathbf{P}(t_k) \triangleq blkdiag\left(\mathbf{P}_{k|k}, \mathbf{Q}(t_k), \mathbf{R}_{k+1}\right) \tag{26}
$$

The Sigma Points ${}^{a}\mathcal{X}^{i}(t_k) \in \mathbb{R}^{n_a}$ of the augmented vector are calculated by

$$
\mathcal{X}^{0} = \bar{\mathbf{x}} \tag{27}
$$

$$
\mathcal{X}^{j} = \bar{\mathbf{x}} + \sqrt{n+\kappa}\left(\sqrt{\mathbf{P}^{X}}\right)_{j} \tag{28}
$$

$$
\mathcal{X}^{j+n} = \bar{\mathbf{x}} - \sqrt{n+\kappa}\left(\sqrt{\mathbf{P}^{X}}\right)_{j} \tag{29}
$$

for $j = 1, \ldots, n$, and where κ is a scale parameter defined by $\kappa = 3 - n$.

Also, to improve the approximation, the Sigma Points are weighted. This weighing process makes the approximation favor some points, such as the mean, more than others. The weights, denominated here by the greek letter ρ are calculated by:

$$
\rho^{0} = \frac{\kappa}{n+\kappa} \tag{30}
$$

$$
\rho^{j} = \frac{1}{2(n+\kappa)} \tag{31}
$$

for $j = 1 \ldots, 2n_a$.

After obtaining the Sigma Points, they can be transformed by considering them as initial conditions in the integration, from t_k to t_{k+1}, of the ODEs:

$$
\dot{\mathcal{X}}^{i}(t) = \mathbf{f}\left(\mathcal{X}^{i}(t), \mathbf{u}(t_k)\right) + \mathbf{g}\left(\mathcal{X}^{i}(t)\right)\mathcal{W}^{i}(t_k) \tag{32}
$$

This integration provides the Sigma Points $\mathcal{X}^{i}_{k+1|k}$ of the predictive state, for $i = 0 \ldots, 2n_a$. It is important to consider that $\mathbf{u}(t)$ and $\mathcal{W}^{i}(t)$ remain constant throughout the integration time interval.

The Sigma Points $\mathcal{X}^{i}_{k+1|k}$ and $\mathcal{V}^{i}_{k+1|k}$, when transformed by equation (8), give rise to the Sigma Points of the predictive measure:

$$
\mathcal{Y}^{i}(t) = \mathbf{h}_{k+1}\left(\mathcal{X}^{i}_{k+1|k}\right) + \mathcal{V}^{i}_{k+1|k} \tag{33}
$$

for $i = 0 \ldots, 2n_a$.

With the aforementioned values, it is possible to approximate, by sample statistics, the predictive expected values on the predictive Sigma Points by calculating

$$\hat{\mathbf{x}}_{k+1|k} \approx \sum_{i=0}^{2n_a} \rho^i \mathcal{X}^i_{k+1|k} \tag{34}$$

$$\hat{\mathbf{y}}_{k+1|k} \approx \sum_{i=0}^{2n_a} \rho^i \mathcal{Y}^i_{k+1|k} \tag{35}$$

$$\mathbf{P}_{k+1|k} \approx \sum_{i=0}^{2n_a} \rho^i \left(\mathcal{X}^i_{k+1|k} - \hat{\mathbf{x}}_{k+1|k}\right)\left(\mathcal{X}^i_{k+1|k} - \hat{\mathbf{x}}_{k+1|k}\right)^T \tag{36}$$

$$\mathbf{P}^Y_{k+1|k} \approx \sum_{i=0}^{2n_a} \rho^i \left(\mathcal{Y}^i_{k+1|k} - \hat{\mathbf{y}}_{k+1|k}\right)\left(\mathcal{Y}^i_{k+1|k} - \hat{\mathbf{y}}_{k+1|k}\right)^T \tag{37}$$

$$\mathbf{P}^{XY}_{k+1|k} \approx \sum_{i=0}^{2n_a} \rho^i \left(\mathcal{X}^i_{k+1|k} - \hat{\mathbf{x}}_{k+1|k}\right)\left(\mathcal{Y}^i_{k+1|k} - \hat{\mathbf{y}}_{k+1|k}\right)^T \tag{38}$$

Similarly to the EKF procedure, the update step of the UKF is carried out by computing equations (20)-(22), but using the predictive data obtained by the equations above.

3.1 UKF Simulations

Equivalently to the previous experiment, the Unscented Kalman Filter was implemented on 100 realizations of the system performance, described by equation (1). Through equations (25)-(38), assuming the initial estimation states $\mathbf{x}_{1|1} = \bar{\mathbf{x}}$ and initial estimation error covariance $\mathbf{P}_{1|1} = \bar{\mathbf{P}}$, the estimation errors obtained are illustrated in Figures 3a to 3f.

The matrix $P_{k|k}$, updated along with the states estimation every iteration, represents the covariance matrix of the estimation error. Therefore, its square root represents the standard deviation matrix of the estimation error. The calculation the matrix square root of $P_{k|k}$ was also plotted in Figures 1a to 1f as green thick dashed lines.

From Figures 3a to 3c, it is possible to see, again, that the error estimations don't always converge to zero and stay mainly outside of the envelope formed by the standard deviation lines. As mentioned before, as these are approximately optimal estimations, convergence might demand the tuning of the covariance matrices.

3.2 UKF with tuned matrices

A similar alteration of matrix $\mathbf{R}$ was adopted, changing it to $\mathbf{R}_{ukf} = blkdiag(100 \times \mathbf{Q}^{ac}, 0.1 \times \mathbf{Q}^{mg})$. The simulation with the altered covariance matrix generated the graphs illustrated in figures 4a to 4f.

With the same goal as before, the tuning of the matrix provided the desired convergence of the estimation errors to zero in every realization.

The analysis of the effects of linearization is analogous to the one made for the EKF in the previous section.

Although theoretically better than the EKF, the Unscented Kalman Filter requires a considerable amount of computational power. This time, when running on the same computer, the UKF algorithm took approximately 325 seconds to run the full system simulation and state estimation.

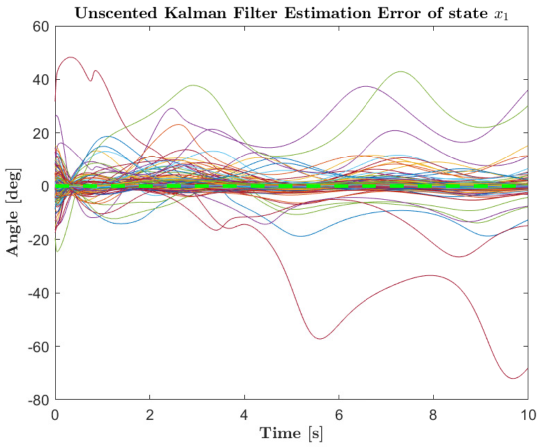

(a) $\tilde{x}_1$

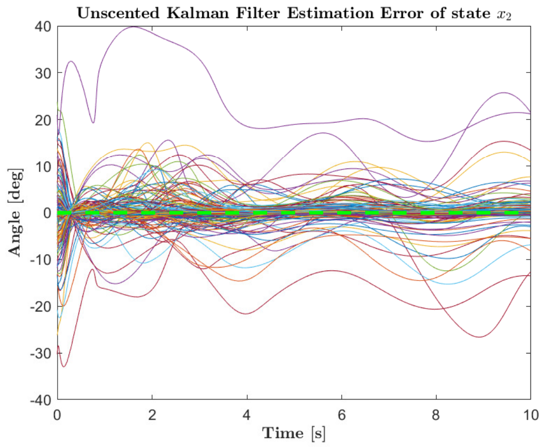

(b) $\tilde{x}_2$

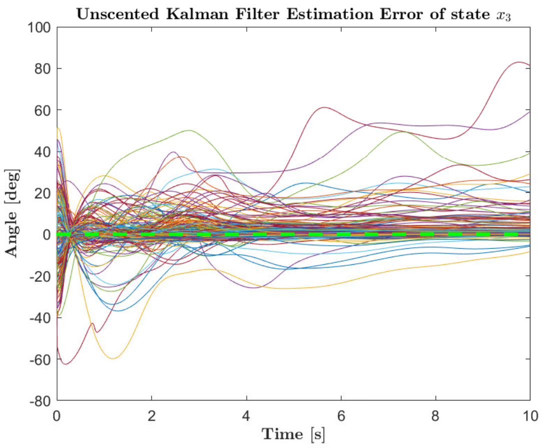

(c) $\tilde{x}_3$

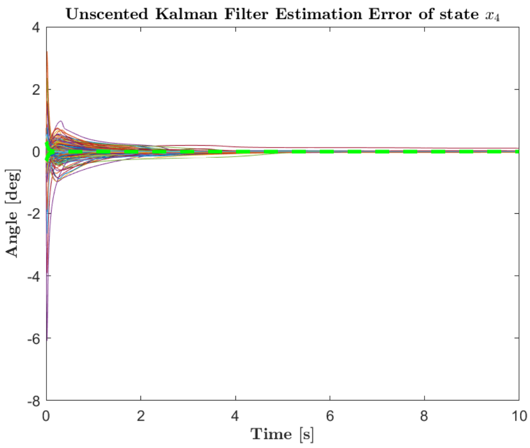

(d) $\tilde{x}_4$

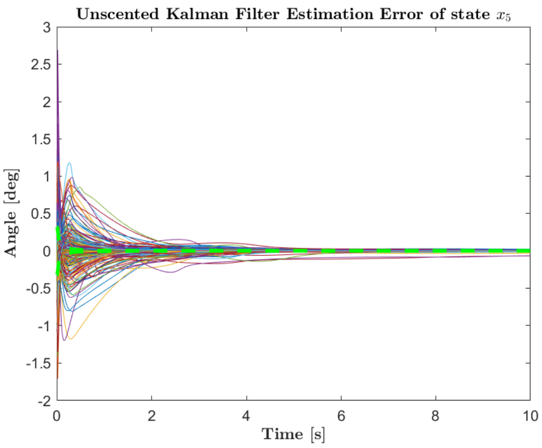

(e) $\tilde{x}_5$

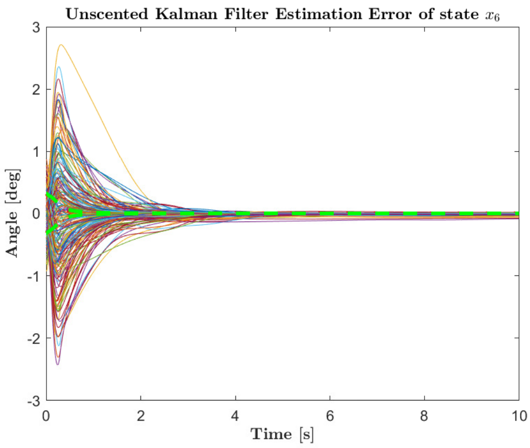

(f) $\tilde{x}_6$

Figure 3: Estimation Error of States x_1 to x_6 with a Unscented Kalman Filter

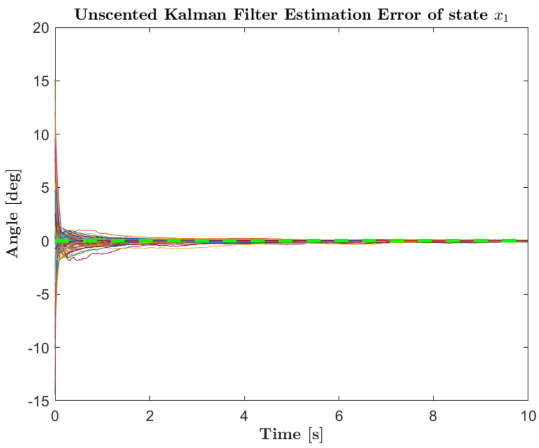

(a) $\tilde{x}_1$

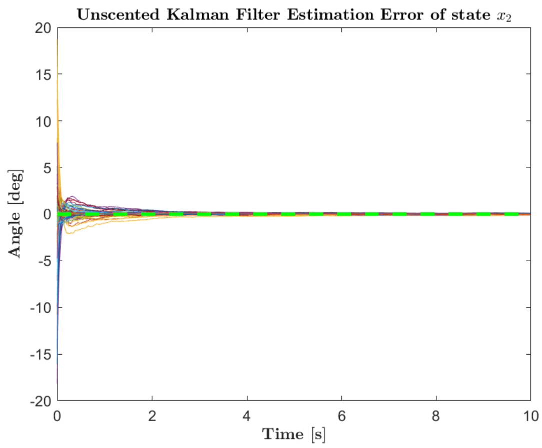

(b) $\tilde{x}_2$

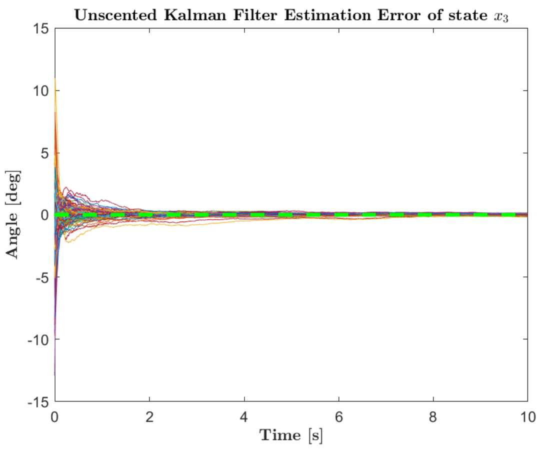

(c) $\tilde{x}_3$

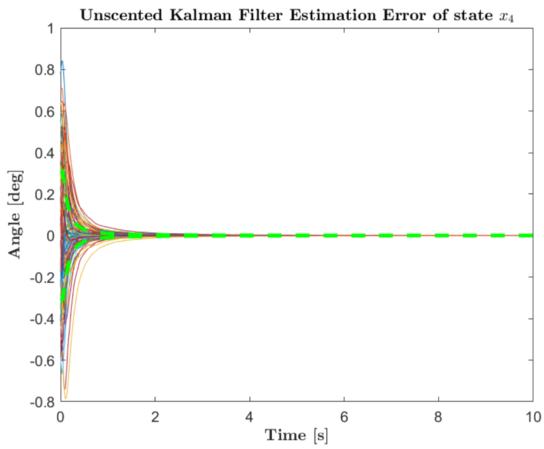

(d) $\tilde{x}_4$

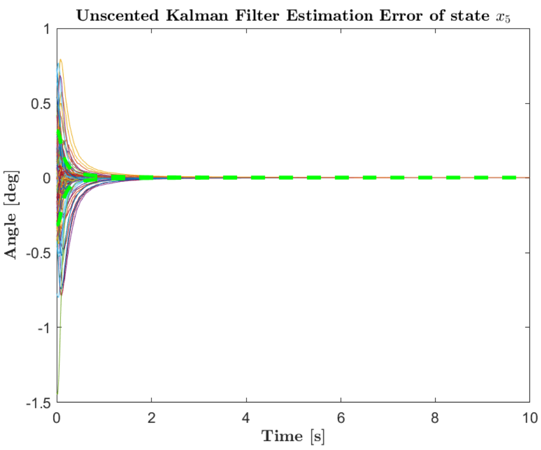

(e) $\tilde{x}_5$

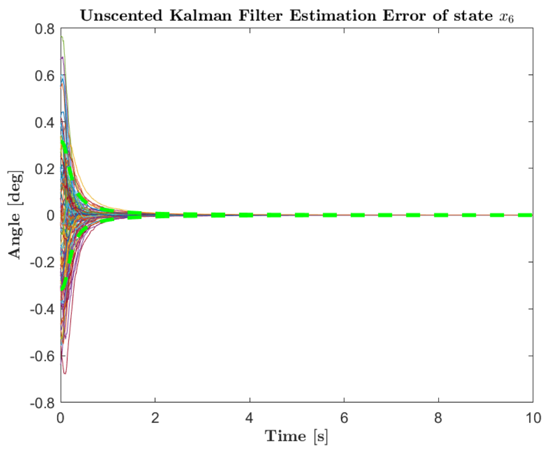

(f) $\tilde{x}_6$

Figure 4: Estimation Error of States x_1 to x_6 with an Unscented Kalman Filter and a modified $\mathbf{R}$ matrix.

4 Conclusion

The objective of this exercise was to formulate an algorithm capable of representing the non-linear attitude determination system of equations of a MAV and estimate its states by using an Extended Kalman Filter and a Unscented Kalman Filter. The simulations were successful and the estimator provided good estimations of $\mathbf{x}$, which was proved by the estimation error $\tilde{\mathbf{x}}$ having low variation around its approximately zero mean, for both estimators. Ideally, the mean and variation of the estimation error would both be zero. But the fact that the system had to be linearized to fit in the filters procedures, along with the existence of added state disturbances and measurement noises in the form of $\mathbf{w}$ and $\mathbf{v}$, respectively, reduces the precision of the estimation. Although the calculations provided a converging filter, the estimation errors of the Euler angles did not stay inside the limits drawn by the standard deviation. The distance between the estimation means and zero was attenuated by tuning R in the filter calculations, but it could not be cancelled. Also, little difference could be observed when comparing the behavior of the states when estimated by an EKF or a UKF.